

# A Spitzer View of Massive Galaxies at $z \sim 1 - 3$

Casey Papovich\* and the GOODS and MIPS GTO teams

Steward Observatory, 933 N. Cherry Ave., Tucson, Arizona, 85721, USA

Received 2005 month day; accepted 2006 month day

**Abstract** I discuss constraints on star-formation and AGN activity in massive galaxies at  $z \sim 1-3$  using observations from the *Spitzer* Space Telescope at 3–24  $\mu\text{m}$ . In particular I focus on a sample of distant red galaxies (DRGs) with  $J - K_s > 2.3$  in the southern Great Observatories Origins Deep Survey (GOODS-S) field. Based on their ACS (0.4–1  $\mu\text{m}$ ), ISAAC (1–2.2  $\mu\text{m}$ ), and IRAC (3–8  $\mu\text{m}$ ) photometry, the DRGs have typical stellar masses  $\mathcal{M} \gtrsim 10^{11} \mathcal{M}_\odot$ . Interestingly, the majority ( $\gtrsim 50\%$ ) of these objects have 24  $\mu\text{m}$  detections, with  $f_\nu(24\mu\text{m}) \geq 50 \mu\text{Jy}$ . If attributed to star formation, then this implies star-formation rates (SFRs) of  $\simeq 100-1000 \mathcal{M}_\odot \text{ yr}^{-1}$ . Thus, massive galaxies at  $z \sim 1.5-3$  have specific SFRs equal to or exceeding the global average value at that epoch. In contrast, galaxies with  $\mathcal{M} \geq 10^{11} \mathcal{M}_\odot$  at  $z \sim 0.3-0.75$  have specific SFRs less than the global average, and more than an order of magnitude lower than that at  $z \sim 1.5-3$ . Thus, the bulk of assembly of massive galaxies is largely complete by  $z \sim 1.5$ . At the same time, based on the X-ray luminosities and near-IR colors, as many as 25% of the massive galaxies at  $z \gtrsim 1.5$  host AGN, implying that the growth of supermassive black holes coincides with massive-galaxy assembly. Lastly, the analysis of high-redshift galaxies depends on bolometric corrections between the observed *Spitzer* 24  $\mu\text{m}$  data and total IR luminosity. I review some of the sources of the (significant) uncertainties on these corrections, and discuss improvements for the future.

**Key words:** galaxies: evolution — galaxies: formation — galaxies: high-redshift — galaxies: stellar-content — Infrared: galaxies

## 1 INTRODUCTION

Most ( $\sim 50\%$ ) of the stellar mass in galaxies today formed during the short time between  $z \sim 3$  and 1 (e.g., Dickinson et al. 2003, Rudnick et al. 2003). Although much of this stellar mass density resides in massive galaxies, which appear at epochs prior to  $z \sim 1-2$  (e.g., Bell et al. 2004, McCarthy 2004), it is still unclear when and where the stars in these galaxies formed. It may be that galaxies “downsize”, forming most of their stars in their current configuration at early cosmological times, with lower mass galaxies continuing to form stars to the present epoch (e.g., Bauer et al. 2005, Juneau et al. 2005). Alternatively, stars may form predominantly in low-mass galaxies at high redshifts, which then merge over time to form large, massive galaxies at more recent times (Bauer et al. 1998, Kauffmann & Charlot 1998, Cimatti et al. 2002).

Understanding the formation and evolution of massive galaxies has been challenged by difficulties in constructing complete samples of star-forming and massive galaxies at  $z \gtrsim 1$ . Massive galaxies at  $z \lesssim 1$  exist on a fairly prominent red sequence (e.g., Blanton et al. 2003, Bell et al. 2004, Faber et al. 2005), and are largely devoid of ongoing star formation, evolve passively,

---

\* E-mail: papovich@as.arizona.edu

and contain up to half of the stellar-mass density. However, current hierarchical models predict colors for massive galaxies at  $z \sim 0$  that are too blue compared to observations (e.g., Somerville, Primack, & Faber 2001, Davé et al. 2005). Some recent models suppress star formation at late times in massive galaxies by truncating star formation at some mass threshold, or by using feedback from strong AGN (e.g., Granato et al. 2001, Davé et al. 2005, Croton et al. 2006). Most of the massive galaxies at  $z \lesssim 1$  have red colors with formation epochs  $z_f \gtrsim 2$ . The morphologies of the most optically luminous (and most massive) galaxies transforms from “normal” early-type galaxies at  $z \sim 1$  to irregular systems at  $z \sim 2-3$  (e.g., Papovich et al. 2005). Therefore, we need to study the properties of massive galaxies at these earlier epochs.

In these proceedings, I discuss recent *Spitzer* observations at  $3-24 \mu\text{m}$  of massive galaxies at  $z \sim 1.5-3$  in the southern Great Observatories Origins Deep (GOODS-S) field. The *Spitzer* IRAC and MIPS observations provide constraints on the star-formation and AGN activity in massive galaxies at these epochs. I discuss implications the analyses of these data have for the stellar-mass assembly rates and formation epochs of massive galaxies. I also review some the uncertainties on these bolometric corrections between the observed *Spitzer*  $24 \mu\text{m}$  data and total IR luminosities in  $z \sim 1.5-3$  galaxies and prospects for future improvements.

## 2 STELLAR MASSES AND STAR FORMATION IN HIGH- $Z$ MASSIVE GALAXIES

GOODS is a multiwavelength survey of two  $10' \times 15'$  fields, one in the northern *Hubble* Deep Field, and one in the southern *Chandra* Deep Field. The GOODS datasets include (along with other things) *HST*/ACS and VLT/ISAAC imaging (Giavalisco et al. 2004), and recent *Spitzer* imaging. I make use of these data for the work described here, as well as data from *Spitzer*/MIPS  $24 \mu\text{m}$  in this field from time allocated to the MIPS GTOs (e.g., Papovich et al. 2004).

In these proceedings, I primarily focus on so-called distant red galaxies (DRGs) selected with  $J - K_s > 2.3$  mag (see Franx et al. 2003). This color criterion identifies both galaxies at  $z \sim 2-3.5$  whose light is dominated by a passively evolving stellar population older than  $\sim 250$  Myr (i.e., with a strong Balmer/4000 Å break between the  $J$  and  $K_s$ -bands), and also star-forming galaxies at these redshifts whose light is heavily reddened by dust (Förster-Schreiber et al. 2004, Labbé et al. 2005, Papovich et al. 2006). For the GOODS-S data, the  $J - K_s > 2.3$  mag selection is approximately complete to stellar mass  $\mathcal{M} \geq 10^{11} M_\odot$  for passively evolving galaxies, and we find 153 DRGs to  $K_s \leq 23.2$  mag, spanning  $0.8 \leq z \leq 3.7$  with  $\langle z \rangle \simeq 2.2$  (see Papovich et al. 2006).

More than 50% of the DRGs have  $24 \mu\text{m}$  detections with  $f_\nu(24\mu\text{m}) \geq 50 \mu\text{Jy}$ . Daddi et al. (2005) find a similar  $24 \mu\text{m}$ -detection rate for massive galaxies at  $1.5 \lesssim z \lesssim 2.5$  selected via their  $BzK$  colors. Interestingly, this implies that the majority of massive galaxies at  $z \sim 2$  emit strongly in the thermal IR — *they are either actively forming stars, supermassive blackholes, or both at this epoch*. The  $24 \mu\text{m}$  emission at  $z \sim 1.5-3$  probes the mid-IR ( $\sim 5-10 \mu\text{m}$ ), which broadly correlates with the total IR,  $L_{\text{IR}} \equiv L(8-1000\mu\text{m})$  (Chary & Elbaz 2001). Figure 1 shows the inferred  $L_{\text{IR}}$  for the DRGs using the Dale et al. (2002) models to convert the observed mid-IR to total IR luminosity. There is inherent uncertainty in this conversion, which I discuss in § 3. The  $24 \mu\text{m}$  flux densities for the  $z \sim 1.5-3$  DRGs yield  $L_{\text{IR}} \approx 10^{11.5-13} L_\odot$ , which if attributed to star-formation corresponds to SFRs of  $\approx 100-1000 M_\odot \text{ yr}^{-1}$  (e.g., Kennicutt 1998).

Nearly all of the DRGs are detected in the deep *Spitzer*/IRAC data, implying they have substantial stellar masses. In Papovich et al. (2006), we modeled the DRG stellar populations by comparing their ACS, ISAAC, and IRAC [ $3.6\mu\text{m}$ ] [ $4.5\mu\text{m}$ ] photometry to a suite of stellar-population synthesis models (Bruzual & Charlot 2003), varying the age, star-formation history,

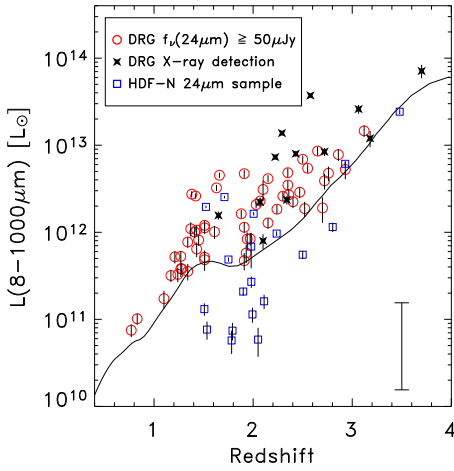


**Fig. 1** Total IR luminosities,  $L_{\text{IR}} \equiv L(8 - 1000)$ , of galaxies inferred from their observed  $24 \mu\text{m}$  emission. Red circles show the values for the DRGs; black stars show those objects with X-ray detections. Blue squares show objects from the HDF-N data (see Papovich et al. 2006). The solid line denotes the  $24 \mu\text{m}$  50% completeness limit. The inset error bar shows the estimated systematic error,  $\approx 0.5$  dex.

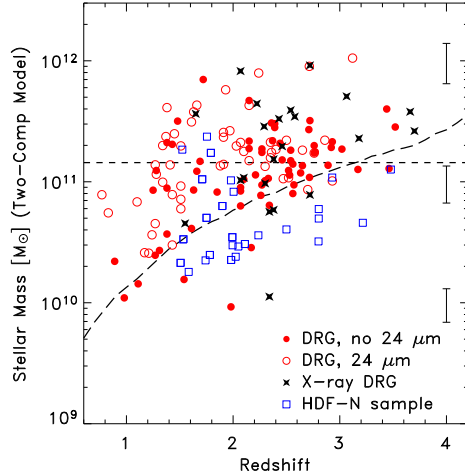


**Fig. 2** Stellar masses of galaxies inferred by fitting two-component models to the galaxies’ rest-frame UV-to-near-IR data. The inset bars show the mean errors as a function of mass. The short-dashed line shows the characteristic present-day stellar mass (Cole et al. 2001); the long-dashed line shows the stellar mass limit for a passively evolving stellar population formed at  $z \sim \infty$  with  $K_s = 23.2$  mag.

and dust content. We use the model stellar-mass-to-light ratios to estimate the galaxies’ stellar mass. We first allow for star-formation histories with the SFR parameterized as a decaying exponential with an  $e$ -folding time,  $\tau$ , ranging from short  $\tau$ ’s (burst of star-formation) to long  $\tau$ ’s (constant star-formation). We also use models with a two-component star-formation history characterized by a passively evolving stellar population formed in a “burst” at  $z_{\text{form}} = \infty$ , summed with the exponentially-decaying-SFR model. Although the modeling loosely constrains the ages, dust content, and star-formation histories of the DRGs, it provides relatively robust estimates of the galaxies’ stellar masses (see also Förster-Schreiber et al. 2004). Typical uncertainties for the stellar masses for the full DRG sample are 0.1–0.3 dex. Figure 2 shows the stellar masses inferred for the DRGs by fitting the two-component models.

Figure 3 shows the specific SFRs ( $\Psi/\mathcal{M}$ ) derived from the masses and SFRs for the DRGs, where the SFRs are calculated from the summed UV and IR emission. The figure also shows the specific SFRs for galaxies at lower redshift from COMBO-17 (Wolf et al. 2003), which overlaps with the GTO *Spitzer*  $24 \mu\text{m}$  imaging. The SFRs for the COMBO-17 galaxies are calculated in an analogous manner as for the DRGs. The massive DRGs at  $1.5 \leq z \leq 3$  have high specific SFRs: DRGs with  $\mathcal{M} > 10^{11} \mathcal{M}_{\odot}$  and  $1.5 \leq z \leq 3$  have  $\Psi/\mathcal{M} \sim 0.2\text{--}10 \text{ Gyr}^{-1}$  (excluding X-ray sources). In contrast, at  $z \lesssim 0.75$  there is an apparent lack of galaxies with high specific SFRs and high stellar masses: galaxies with  $\mathcal{M} \geq 10^{11} \mathcal{M}_{\odot}$  have  $\Psi/\mathcal{M} \sim 0.1\text{--}1 \text{ Gyr}^{-1}$ .

We define the integrated specific SFR as the ratio of the sum of the SFRs,  $\Psi_i$ , to the sum of their stellar masses,  $\mathcal{M}_i$ ,  $\Upsilon \equiv \sum_i \Psi_i / \sum_i \mathcal{M}_i$ , summed over all  $i$  galaxies. This is essentially just the ratio of the SFR density to the stellar mass density for a volume-limited sample of galaxies. Figure 4 shows the integrated specific SFRs for DRGs at  $z \sim 1.5\text{--}3.0$  and COMBO-17 at  $z \sim 0.4$  and  $0.7$  with  $\mathcal{M} \geq 10^{11} \mathcal{M}_{\odot}$  (see Papovich et al. 2006). The data point for the DRGs includes all objects with  $\mathcal{M} \geq 10^{11} \mathcal{M}_{\odot}$ , and assumes that  $24 \mu\text{m}$ -undetected DRGs have no star

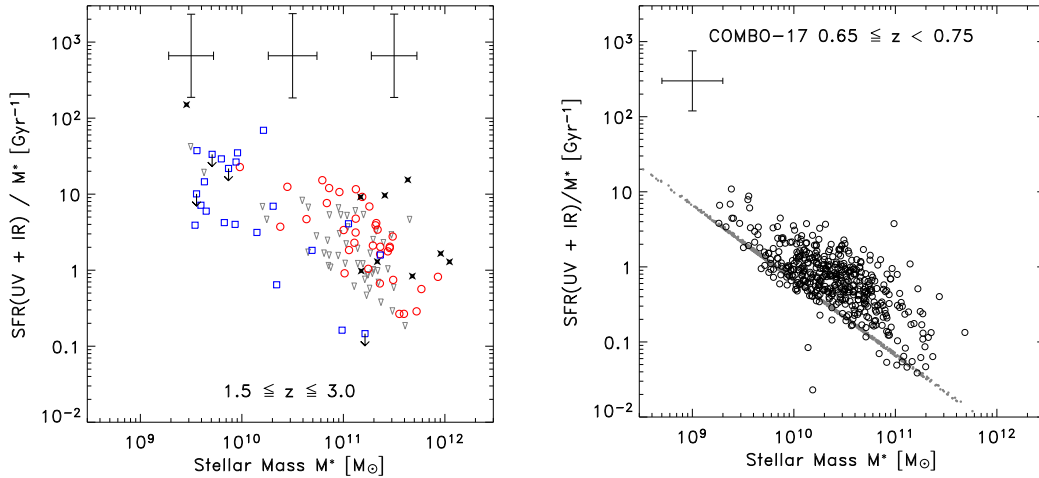


**Fig. 3** The specific SFR as a function of galaxy stellar mass. The Left panel shows the DRG and HDF-N galaxies with  $1.5 \leq z \leq 3$ , with symbols the same as in figure 1. The Right panel shows galaxies from COMBO-17 (as labeled). Open circles show COMBO-17 galaxies with  $24 \mu\text{m}$  detections, small filled symbols show upper limits for galaxies undetected at  $24 \mu\text{m}$ .

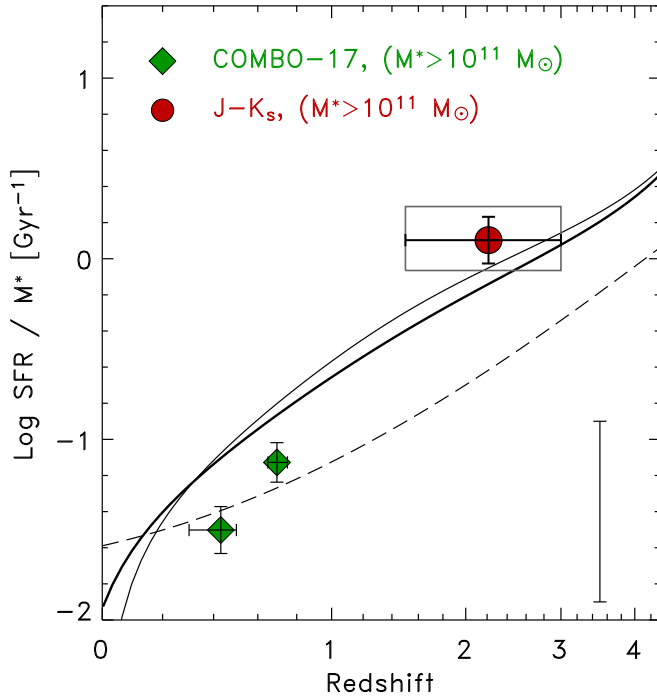
formation. The error-box lower bound shows what happens if we exclude objects with X-ray detections or IR colors indicative of AGN. The error-box upper bound shows what happens if we calculate SFRs for the  $24 \mu\text{m}$ -undetected DRGs assuming they have  $f_\nu(24\mu\text{m})=60 \mu\text{Jy}$ , the 50% completeness limit. The integrated specific SFR in galaxies with  $\mathcal{M} > 10^{11} M_\odot$  declines by more than an order of magnitude from  $z \sim 1.5-3$  to  $z \lesssim 0.7$ . Our results indicate that the relative star-formation in massive galaxies is reduced for  $z \lesssim 1$  as galaxies with lower stellar masses have higher specific SFRs, supporting the so-called “downsizing” paradigm.

Figure 4 also shows the specific SFR integrated over all galaxies (not just the most massive); this is the ratio of the cosmic SFR density to its integral,  $\Upsilon = \dot{\rho}_* / \int \dot{\rho}_* dt$ . There is a decrease in the global specific SFR with decreasing redshift. The evolution in the integrated specific SFR in massive galaxies is accelerated relative to the global value. Galaxies with  $\mathcal{M} \geq 10^{11} M_\odot$  were forming stars at or slightly above the rate integrated over all galaxies at  $z \sim 1.5-3$ . In contrast, by  $z \lesssim 1$  galaxies with  $\mathcal{M} \geq 10^{11} M_\odot$  have an integrated specific SFR much lower than the global value. *Thus, by  $z \lesssim 1.5$  massive galaxies have formed most of their stellar mass, and lower-mass galaxies dominate the cosmic SFR density* (see also Papovich et al. 2006).

### 3 UNCERTAINTIES ON MID-IR-DERIVED IR LUMINOSITIES

#### 3.1 AGN Contribution to the mid-IR Emission

Many of the massive galaxies at  $z \sim 1.5-3$  are detected in the deep X-ray data. In figures 1 and 3, the X-ray-detected DRGs tend to have the highest inferred IR luminosities and specific SFRs. Many of these objects have  $L_{\text{IR}} \geq 10^{13} L_\odot$ , comparable to PG quasars, which have warm thermal dust temperatures (Haas et al. 2003). The X-ray to optical flux ratios in these objects imply the presence of an AGN with  $L_X \gtrsim 10^{42} \text{ erg s}^{-1}$  (for  $z \gtrsim 1.5$ , see Alexander et al. 2003, Papovich et al. 2006). In addition, many authors are finding AGN candidates based on rest-frame near-IR colors from *Spitzer* observations. The X-ray, UV, and optical emission in these AGN is heavily obscured by gas and dust, and they are often missed in deep X-ray surveys (e.g., Donley et al. 2005, Stern et al. 2005, Alonso-Herrero et al. 2006, Barmby et al. 2006). Roughly



**Fig. 4** Evolution of the integrated specific SFR, the ratio of the total SFR to the total stellar mass (from Papovich et al. 2006). The curves show the expected evolution from the global SFR density (solid lines, Cole et al. 2001, thick line includes correction for dust extinction; dashed line, Hernquist & Springel 2003). Data points show results for galaxies with  $\geq 10^{11} M_{\odot}$ . Filled circle corresponds to the DRGs; filled diamonds correspond to the COMBO-17 galaxies. The inset error bar shows an estimate on the systematics.

25% of the non-X-ray detected DRGs in the GOODS-S field satisfy the IRAC color-selection for AGN from Stern et al. (2005). Of these, roughly one-half have ACS-through-IRAC colors consistent with dust-enshrouded AGN. Figure 5 shows examples of these galaxies with and without X-ray detections. In all cases, the galaxies show a clear flux excess in their IRAC [5.8 $\mu$ m] and [8.0 $\mu$ m] photometry, presumably arising from the AGN. Combined with the 15% of DRGs detected in the X-rays, up to 25% of the DRG population host AGN.

If AGN contribute to the observed 24  $\mu$ m emission in galaxies at  $z \sim 1.5-3$ , then they can affect the inferred IR luminosities. For example, although the Chary & Elbaz (2001) and Dale & Helou (2002) IR templates include galaxies with  $L_{\text{IR}} \gtrsim 10^{13} L_{\odot}$ , using an IR template for Mrk 231 — with a known AGN and warmer dust temperature — would reduce the inferred IR luminosity for galaxies at  $z \sim 1.5-3$  by factors of  $\sim 2-5$ . To limit the effects of any bias in the inferred IR luminosities caused by AGN, we restricted the error box on the integrated specific SFR for the DRGs in figure 4 to only those galaxies with no X-ray or IR indications for AGN.

Even when AGN are present, it is unclear whether star-formation or the AGN activity dominates the bolometric IR luminosity. Alexander et al. (2005) demonstrated that a high fraction ( $\sim 80\%$ ) of sub-mm galaxies are detected in 2 Msec *Chandra* X-ray data. However, the X-ray-detected sub-mm galaxies have IR to X-ray luminosity ratios up to an order of magnitude higher than what is expected for AGN alone. This suggests that both star-formation and AGN contribute to the bolometric emission. Similarly, Frayer et al. (2003) report a near-

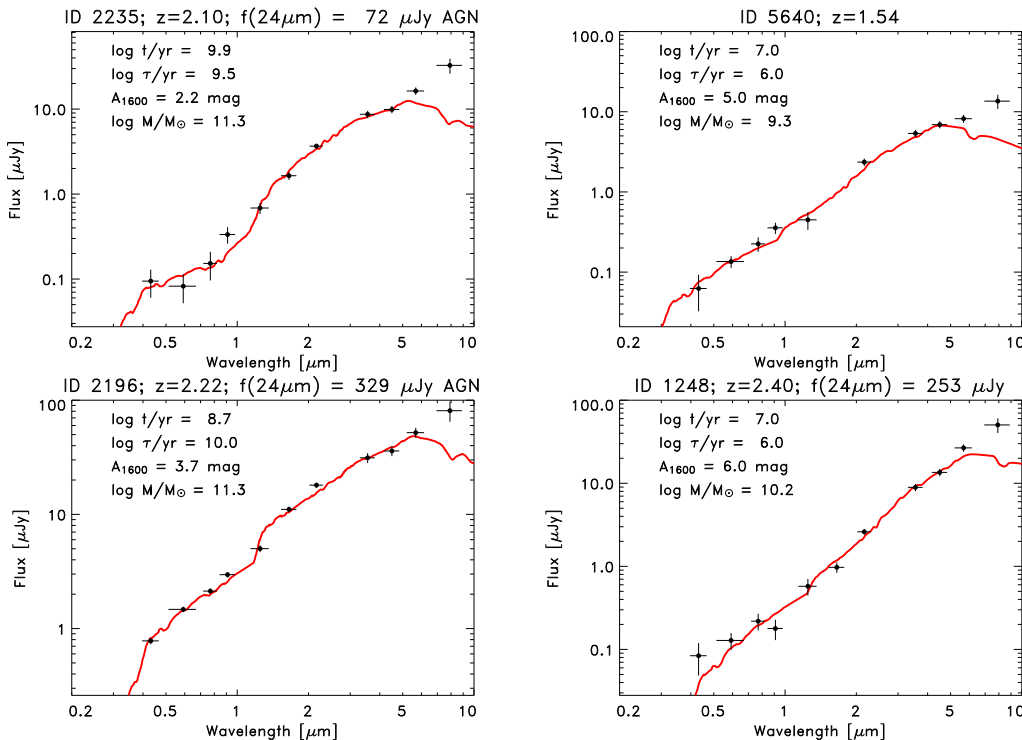


**Fig. 5** SEDs of DRGs with putative AGN. The data points in each panel show the rest-frame UV to near-IR SED from the ACS (0.4–1 $\mu\text{m}$ ), ISAAC (1–2.2 $\mu\text{m}$ ), and IRAC (3–8 $\mu\text{m}$ ) photometry. The solid line shows the best-fit model SED to the ACS, ISAAC, and IRAC [3.6 $\mu\text{m}$ ] and [4.5 $\mu\text{m}$ ] photometry. The two galaxies in the Left panels have X-ray detections, but the two in the Right panels do not. In all cases the galaxies show excess emission in the IRAC [5.8 $\mu\text{m}$ ] and [8.0 $\mu\text{m}$ ] bands, presumably from hot dust near the AGN.

IR spectrum of a sub-mm galaxy SMM J04431+0210 at  $z \sim 2.5$ . This galaxy has  $J - K_s \simeq 3.2 \text{ mag}$ , qualifying as a DRG. The spectrum shows that the galaxy nucleus has a low  $\text{H}\alpha$  to  $[\text{NII}]$  flux ratio consistent with ionization from an AGN. However,  $\text{H}\alpha$  is spatially resolved in their spectrum and the  $[\text{NII}]$  line strength drops off in the off-nucleus spectrum. This implies extended star-formation beyond the nucleus, which presumably contributes to the inferred IR luminosity. Therefore, it seems that both AGN and star-formation occur simultaneously in high-redshift IR-detected galaxies and both probably contribute to the IR emission.

The high AGN occurrence in DRGs and sub-mm galaxies provides some evidence that massive galaxies at  $z \sim 1.5\text{--}3$  simultaneously form stars and grow supermassive black holes. Although speculative, the presence of AGN in these galaxies may provide the impetus for the present-day relation between black hole and bulge mass, and/or provide the feedback necessary to squelch star-formation (e.g., Kauffmann et al. 2004), moving the galaxies onto the red sequence. Emission line ratios from high-resolution spectroscopy at near-IR and/or mid-IR wavelengths may help constrain the ionization state of the galaxies’ gas, identifying the fraction of galaxies with strong AGN activity as a function of mass at these redshifts.

### 3.2 Uncertainties in the Shape of the IR Spectral Energy Distribution

Although the mid-IR (5–15  $\mu\text{m}$ ) emission broadly correlates with the total IR luminosity (e.g., Chary & Elbaz 2001), there exists considerable scatter. Partly this arises because galaxies of a given IR luminosity show a range in the strength of their mid-IR emission (from polycyclic

aromatic hydrocarbons, PAHs) and absorption features (e.g., Armus et al. 2004). This variation is reflected in a comparison of various model IR spectral energy distributions in the literature (e.g., see Le Floc’h et al. 2005). For example, if we used the IR templates of Chary & Elbaz (2001) instead of those of Dale & Helou (2002), then we would derive IR luminosities a factor of 2–3 higher for  $z \sim 1.5$ –3 galaxies with  $L_{\text{IR}} \sim 10^{12.5-13} L_{\odot}$ . In a recent study of galaxies at  $z \leq 1.2$  detected at *ISO* 15  $\mu\text{m}$  and *Spitzer* 24  $\mu\text{m}$  in the northern GOODS field, Marcillac et al. (2006) found that, compared to Chary & Elbaz (2001), the IR models of Dale & Helou (2002) provide a tighter correlation between  $L_{\text{IR}}$  derived from the mid-IR and radio flux densities with a scatter of 40%, suggesting the latter may better reflect reality.

Some scatter is inherent in converting the 24  $\mu\text{m}$  flux densities to total IR luminosity. Several studies of the mid-IR colors of galaxies to  $z \sim 1$  show that their 15 and 16  $\mu\text{m}$  to 24  $\mu\text{m}$  colors have more scatter than predicted by simple models that map a single IR template to a given IR luminosity (e.g., Elbaz et al. 2005, Teplitz et al. 2005, Marcillac et al. 2006). Chapman et al. (2003) find that the temperature–luminosity distribution in local IR–luminous galaxies has a factor of 2–3 scatter in the IR–luminosity for galaxies of a given dust temperature. However, Daddi et al. (2005) found that the Chary & Elbaz (2001) IR model with  $L_{\text{IR}} = 10^{12.2} L_{\odot}$  fits the average spectral energy distribution of 24  $\mu\text{m}$ –detected *BzK* objects at  $\langle z \rangle = 1.9$  in the northern GOODS field. Therefore, *while on average high-redshift galaxies have IR spectral energy distributions consistent with the models, individually there remains significant scatter.*

## 4 SUMMARY

In this contribution, I discussed star-formation and AGN activity in massive galaxies ( $\gtrsim 10^{11} M_{\odot}$ ) at  $z \sim 1$ –3 using observations from the *Spitzer* Space Telescope at 3–24  $\mu\text{m}$ . Interestingly, the majority ( $\gtrsim 50\%$ ) of these objects have  $f_{\nu}(24\mu\text{m}) \geq 50 \mu\text{Jy}$ , which if attributed to star formation implies SFRs of  $\simeq 100$ –1000  $M_{\odot} \text{ yr}^{-1}$ . Galaxies at  $z \sim 1.5$ –3 with  $M \geq 10^{11} M_{\odot}$  have specific SFRs equal to or exceeding the global average value. In contrast, galaxies at  $z \sim 0.3$ –0.75 with these masses have specific SFRs less than the global average, and more than  $10\times$  lower than that at  $z \sim 1.5$ –3. Therefore, by  $z \lesssim 1.5$  massive galaxies have formed most of their stellar mass, and lower-mass galaxies dominate the SFR density.

As many as 25% of the massive galaxies at  $z \gtrsim 1.5$  host AGN. The high AGN occurrence in massive galaxies at  $z \sim 1.5$ –3 provides evidence that they are simultaneously forming stars and growing supermassive black holes. This may provide the impetus for the present-day black-hole–bulge-mass relation and/or provide the feedback necessary to squelch star-formation in such galaxies, moving them onto the red sequence.

The largest source of uncertainty results from systematic errors on the bolometric corrections between the observed *Spitzer* 24  $\mu\text{m}$  data and total IR luminosity. While on average high-redshift galaxies have IR spectral energy distributions consistent with the models, individually there remains significant scatter. Future work is needed to improve our understanding of the distribution between the mid-IR (rest-frame 5–15  $\mu\text{m}$ ) emission and total IR luminosity in galaxies at  $z \sim 1.5$ –3. It may be possible to use “average” 24-to-70 and 160  $\mu\text{m}$  colors of distant galaxies to further constrain the distribution and scatter of galaxies’ IR spectral energy distributions. The upcoming *Herschel* Space Observatory (and eventually *SAFIR*) will mitigate this problem by measuring the far-IR emission of distant galaxies directly.

**Acknowledgements** I wish to thank the conference organizers for their hard work in planning an outstanding meeting in an extremely beautiful locale. I look forward to the next “Extreme Starbursts” meeting. I am grateful for my colleagues on the MIPS GTO and GOODS teams for this research; I am

thankful for their continued collaboration. In particular I am indebted to L. Moustakas, M. Dickinson, E. Le Floch, E. Daddi, and G. Rieke. I also am grateful for the AAS International Travel Grant, which made the trip to this meeting possible. Support for this work was provided by NASA through the Spitzer Space Telescope Fellowship Program, through a contract issued by the Jet Propulsion Laboratory (JPL), California Institute of Technology (Caltech) under a contract with NASA.

## References

- Alexander, D. M., Bauer, F. E., Brandt, W. N., et al. 2003, *AJ*, 126, 539
- Alexander, D. M., Bauer, F. E., Chapman, S. C., et al. 2005, *ApJ*, 632, 736
- Alonso-Herrero, A., et al. 2006, *ApJ*, in press (astro-ph/0511507)
- Armus, L., Charmandaris, V., Spoon, H. W. W., et al. 2004, *ApJS*, 154, 178
- Barmby, P., Alonso-Herrero, A., Donley, J. L., et al. 2006, *ApJ*, in press (astro-ph/0512618)
- Bauer, A. E., Drory, N., Hill, G. J., & Feulner, G. 2005, *ApJ*, 621, L89
- Bauer, C. M., Cole, S., Frenk, C. S., & Lacey, C. G. 1998, *ApJ*, 498, 504
- Bell, E. F., Wolf, C., Meisenheimer, K., et al. 2004, *ApJ*, 608, 752
- Blanton, M. R., Hogg, D. W., Bahcall, N. A., et al. 2003, *ApJ*, 594, 186
- Bruzual, G. A., & Charlot, S. 2003, *MNRAS*, 344, 1000
- Calzetti, D., Armus, L., Bohlin, R. C., et al. 2000, *ApJ*, 533, 682
- Chapman, S. C., Helou, G., Lewis, G. F., & Dale, D. A. 2003, *ApJ*, 588, 186
- Chary, R. R., & Elbaz, D. 2001, *ApJ*, 556, 562
- Cimatti, A., Daddi, E., Mignoli, M., et al. 2002, *A&A*, 381, L68
- Cole, S., Norberg, P., Baugh, C. M., et al. 2001, *MNRAS*, 326, 255
- Croton, D., Springel, V., White, S. D. M., et al. 2006, *MNRAS*, 365, 11
- Daddi, E., Dickinson, M., Chary, R., et al. 2005b, *ApJ*, 631, L13
- Dale, D. A., & Helou, G. 2002, *ApJ*, 576, 159
- Davé, R., Finlator, K., Hernquist, L., et al. 2005, preprint (astro-ph/0510625)
- De Lucia, G., Springel, V., White, S. D. M., et al. 2005, preprint (astro-ph/0509725)
- Dickinson, M., Papovich, C., Ferguson, H. C., & Budavári, T. 2003, *ApJ*, 587, 25
- Donley, J. L., Rieke, G. H., Rigby, J. R., Pérez-Gonzalez, P. G. 2005, *ApJ*, 634, 169
- Elbaz, D., Le Floch, E., Dole, H., & Marcellac, D., 2005 *A&A*, 434, 1
- Faber, S. M., Willmer, C. N. A., Wolf, C., et al. 2005, preprint (astro-ph/0506044)
- Förster-Schreiber, N. M., van Dokkum, P. G., Franx, M., et al. 2004, *ApJ*, 616, 40
- Franx, M., Labbé, I., Rudnick, G., et al. 2003, *ApJ*, 587, 79
- Fruer, D., Armus, L., Scoville, N. Z., et al. 2003, *ApJ*, 126, 73
- Giavalisco, M., Dickinson, M., Ferguson, H. C., et al. 2004, *ApJ*, 600, L93
- Granato, G. L., Silva, L., Monaco, P., et al. 2001, *MNRAS*, 324, 757
- Haas, M., Klaas, U., Müller, S. A. H., et al. 2003, *A&A*, 402, 87
- Juneau, S., Glazebrook, K., Crampton, D., et al. 2005, *ApJ*, 619, L135
- Kauffmann, G., & Charlot, S. 1998, *MNRAS*, 294, 705
- Kauffmann, G., White, S. D. M., Heckman, T. M., et al. 2004, *MNRAS*, 353, 713
- Kennicutt, R. C., Jr. 1998, *ARA&A*, 36 189
- Labbé, I., Huang, J., Franx, M., et al. 2005, *ApJ*, 624, L81
- Le Floch, E., Papovich, C., Dole, H., et al. 2005, *ApJ*, 632, 169
- Marcellac, D., Elbaz, D., Chary, R., et al. 2006, *A&A*, in press
- McCarthy, P. 2004, *ARA&A*, 42, 477
- Papovich, C., Dole, H., Egami E., et al. 2004, *ApJS*, 154, 70
- Papovich, C., Dickinson, M., Giavalisco, M., Conselice, C. J., & Ferguson, H. C. 2005, *ApJ*, 631, 101
- Papovich, C., Moustakas, L. A., Dickinson, M., et al. 2006, *ApJ*, in press (astro-ph/0511289)
- Rudnick, G., Rix, H.-W., Franx, M., et al. 2003, *ApJ*, 599, 847



- Stern, D., Eisenhardt, P., Gorjian, V., et al. 2005, ApJ, 631, 163  
Somerville, R. S., Primack, J., & Faber, S. M. 2001, MNRAS,  
Teplitz, H., Charmandaris, V., Chary, R., et al. 2005, ApJ, 634, 128  
Wolf, C., Meisenheimer, K., Rix, H.-W., et al. 2003, A&A, 401, 73